Evaluation of the internal quality of pomegranates using noninvasive visible/near infrared transmittance spectroscopy

António Brázio[1], Ana M. Cavaco[1], M. Dulce Antunes[1,2] & Rui Guerra[1]

[1]CEOT, Universidade do Algarve, Campus de Gambelas, 8005-189 Faro, Portugal. rguerra@ualg.pt
[2]MeditBio, Centro para os Recursos Biológicos e Alimentos Mediterrânicos, Universidade do Algarve, Campus de Gambelas, 8005-189 Faro, Portugal. mantunes@ualg.pt

Abstract

The purpose of this research was to evaluate the possibility of determining the internal quality of pomegranates (*Punica granatum* L.) using noninvasive spectroscopic methods. We used VIS/NIR (Visible, Near Infrared) transmittance spectroscopy because of its speed of execution, the possibility of pre-processing of data in real time and the ease of use in the control process and separation of fruit. A LabVIEW program was developed to control the spectrometer, perform the acquisition and to preprocess the data. The transmittance spectra of thirty pomegranates were measured using two different experimental setups, one where the light is collected with contact with the fruit and another where there is no contact with the fruit. The data was processed and analyzed in R. The absorbance spectra and their first and second derivatives were calculated, normalized and filtered using the Savitzky-Golay filter. Through data analysis we were able to pinpoint some wavelengths of interest that allowed us to build a mathematical model based on a multilinear regression, able to successfully predict the internal conditions of the pomegranates from their transmittance spectra.

Keywords: Spectroscopy, optics, postharvest, mathematical modeling, multilinear regression.

Resumo

Determinação não-invasiva da qualidade interna de romãs com espectroscopia de transmitância no visível e infravermelho próximo. Este trabalho incide sobre o estudo de viabilidade da utilização de métodos não invasivos na determinação da qualidade interna da fruta, mais concretamente, na avaliação da qualidade interna de romãs da variedade Acco (*Punica granatum L.*) através de métodos de espectroscopia de transmitância. Esta técnica é usada na gama do visível e infravermelho próximo devido à rapidez de execução, possibilidade de fazer o pré-processamento em tempo real e, também pela simplicidade no controlo de todo o processo bem como na separação da fruta. O controlo do espectrómetro, a aquisição e pré-processamento dos dados foi executado com um programa em LabVIEW. Os espectros de transmitância de trinta romãs foram medidos em duas configurações experimentais diferentes, uma onde a coleção da luz é feita com contato e outra sem contato com o fruto. O processamento e análise dos dados foi realizado no software R. Através dos espectros de transmitância determinamos os espectros de absorbância, bem como a primeira e a segunda derivada destes, sendo posteriormente filtrados pelo método de Savitzky-Golay. Analisando os dados foi-nos possível determinar comprimentos de onda específicos de interesse, a partir dos quais foi possível construir um modelo matemático baseado numa

regressão linear múltipla capaz de prever a qualidade interna das romãs através dos seus espectros de transmitância.

Palavras-chave: Espectroscopia, ótica, pós-colheita, modelação matemática, regressão linear múltipla.

Introduction

Visible/Near infrared spectroscopy has been applied with significant success to the determination of fruit internal properties in the last decades (Nicolai et al. 2007). The determination of internal defects through transmittance spectroscopy is also a possibility that has been explored, for example in apples (Clark et al. 2003) and pears (Han et al. 2006). One good candidate for internal defect screening by optical methods would be the pomegranate grown in the Algarve region, since the *Alternaria alternata* fungus (Simmons 1967) is causing fruit rot (Tziros et al., 2008). However, this was not yet attempted or, at least described in the literature, essentially because of the opacity of the fruit's skin and of its large dimensions. In view of these constraints, other methods have been tried: internal structure and defects of pomegranates (*Punica granatum* L.) have been assessed through the use of magnetic resonance images (Khoshroo et al. 2009, Zhang et al. 2012) and X-ray computed tomography (Magwaza & Opara 2014). In this work we show that with strong illumination and sensitive detection it was possible to attain encouraging results for the use of NIR transmission spectroscopy in the screening of pomegranate internal structure.

Materials and Methods

Fruit. Thirty pomegranates (*Punica granatum* L. Acco) were supplied by Luís Sabbo Lda. (Tavira, Portugal) in October 2014 and stored at room temperature for 2 days. The fruit were in an advanced stage of maturation but did not show external signs of rot core. The measurements were taken in the second and third days after reception.

The pomegranates were described in terms of the parameters relevant for this study: physical dimensions (height and diameter), colour (pulp and peel), external signs of damages, extension and severity of internal damages. For the internal characteristics we made a longitudinal cut, photographed the two halves, register the pulp colour, the extension and severity of internal damages. The severity of the damage was quantified according to an observer-based scale from 1 to 5, where 1 = no damage, 2 = mild damage, 3 = medium damage, 4 = severe damage and 5 = extremely damaged pomegranate. The damage extension was quantified by the percentage of the affected area in the section cut, in a scale from 0 to 4, where 0 = 0%, 1 = between 0 and 25%, 2 = between 25 and 50%, 3 = between 50 and 75% and 4 = between 75 to 100%.

Experimental setup. The optical setup is shown in figure 1. It consists of a halogen lamp (OSRAM model 64637, OSRAM, Germany) as light source, housed in 2" optical tube. The tube allows for the insertion of two convex lenses with focal lengths 60 and 75 mm that focus the light on a spot of about 3 cm on the pomegranate's surface, located at a distance of 5 cm from the lenses. The light that traverses the fruit is collected in the opposite side by a 600 micron core optical fiber, also about 5 cm away from the fruit surface. The numerical aperture of the fiber (NA = 0.22) defines a cone of acceptance and an observation spot of about 4 cm diameter. The optical fiber is also mounted on a 1" optical tube, mainly for light insulation purposes. The optical fiber is then connected to a spectrometer (Hamamatsu C9405CA, Hamamatsu, Japan), whose spectral response range is from 500 to 1100 nm. The measurements were performed in a dark room.

Two different measurements were made: contact and contactless. In the former the optical tube was put into contact with the fruit. This insured perfect optical isolation but a reduced spot size for light collection of about 25 mm diameter. In the contactless mode a distance of 4 cm was kept between the end of the optical tube and the fruit surface. This increased the diameter of the observation spot to 4 cm, which increased the optical power gathered, but at the same time allowed for possible contamination from light reflected off the fruit peel and by the room walls. The transmittance measurements need a reference. This was obtained using an integrating sphere of 50 mm inner diameter (Ocean Optics ISP-50-8-R-GT, Ocean Optics, USA) and a diffuse reflection standard reflector (Ocean Optics WS-1). It is important to note that the geometry for the reference is not the same as that used for the fruits. This means that the transmittance to be determined is not the true transmittance, but an arbitrarily scaled reflectance. However, this is enough for our purposes. The transmittance spectra were calculated using the expression:

$$T = \frac{S - D}{R - D}, \tag{1}$$

where S is the sample raw spectrum, R, is the reference raw spectrum and D represents the dark signal, that is, the signal measured by the spectrometer in the absence of light.

Data analysis. Data acquisition was carried out through a program written in LabVIEW, which communicated with the spectrometer through the appropriate virtual instruments (VI's). This program was used to control the acquisition parameters (integration time, number of scans, etc.) and collect the readings of the spectrometer. Moreover, it provided us the possibility to assess the spectra in real time to check the quality of the measurements.

The data acquisition procedure had the following sequence: i) adjustment of the optics; ii) check of the reference spectrum intensity; iii) acquisition of the dark spectrum; iv) acquisition of the reference spectrum; v) acquisition of the pomegranates' spectra; vi) new acquisition of dark and reference spectra for consistency check. This procedure was repeated for each lot of ten pomegranates two times, one for each experimental configuration.

The acquired data was processed in R (R Core Team, 2014). After importing the raw spectra, the transmittance spectra were calculated using eq. (1) and normalized (to the maximum value). The spectra were excessively noisy below ~600 nm and above ~1000 nm (depending on the configuration). Using the signal to noise ratio defined as

$$SNR = \frac{\langle S - D \rangle}{\sigma(D)}, \tag{2}$$

where the angled brackets represent average and σ represents the standard deviation, we have performed subsequent calculations only for those wavelengths satisfying SNR > 2, since the others are dominated by noise and do not bear significant information. To obtain the absorbance spectra (μ) we used the following condition:

$$\begin{cases} \mu = 0 & \text{if} \quad SNR < 2 \\ \mu = \frac{1}{d}\log\left(\frac{1}{T}\right) & \text{if} \quad SNR > 2 \end{cases}, \tag{3}$$

where d represents the diameter of the pomegranate. The absorbance spectra was then processed through the Savitzky-Golay (SG) filter (Savitzky & Golay, 1964). This is a digital filter that can be applied to series of digital data to enhance signal to noise ratio without greatly distorting the behavior of the signal through convolution, by fitting successive subsets of adjacent data points with a low-degree polynomial by the method of linear least squares. The result is the filtered absorbance spectra, μ_{SG}. The first and second derivative of μ may also be calculated by the SG filter, which delivers smoothing

and derivation simultaneously. These derivatives of the absorbance spectra are represented in the following by μ'_{SG} and μ''_{SG} respectively.

Results and Discussion

The results from the characterization of the pomegranates in terms of extension and severity of internal damages are shown in table 1. The majority of the fruit exhibited extreme internal damage throughout a large area extension.

The raw spectra of the thirty pomegranates obtained with the two different experimental configurations before their normalization and the normalized transmittance spectra obtained with the equation (1) are shown in figure 2. The contactless configuration yielded a better SNR, especially after 900 nm. This was more evident in the normalized transmittance plot (bottom left). The noisy pattern is the results of having the signal too close to the dark level. The better signal to noise ratio obtained in the contactless configuration is mainly due to the largest observation spot. However, it is possible that the signal is also being boosted by parasitic light reflections from the fruit skin and the dark room walls. This was not further investigated.

The analysis of the contact data did not proceed further due to the lack of quality of the signal. The remaining of the work was performed only on the contactless data. The absorbance spectra were calculated through equation (3) and subsequently filtered with the SG method (figure 3, top). This same filter was used for the calculation of the first and second derivative of the absorbance spectra (figure 3, bottom).

The top plots depicted in figure 3 show a common behavior in fruit VIS/NIR spectra: the different lines seem to be vertically translated relatively to each other. This is mainly caused by different scattering levels within the fruit. There are several techniques to partially compensate for this effect and we have adopted the more classical one: the consecutive application of log (in the absorbance definition) and derivative cancels the effect of multiplicative constants (and the scattering effect is presumably a multiplicative effect). The net effect, observed in the bottom plots of figure 3, is that the importance of the relative shift among the spectra was diminished while the slight differences in the curves' slopes were enhanced.

Multilinear regression is a multivariate statistical technique for examining linear correlations between two or more independent variables and a single dependent variable. A thorough analysis of all the spectra enabled us to pinpoint several wavelengths of interest (table 2) that allowed the building of a mathematical model with the *lm()* (linear model) R function. These wavelengths and some relations between them were used as the independent variables for the multilinear regression. Thus obtaining a multilinear model of the first order described by the following equation,

$$severity = -196,475 \cdot T_{837} + 119,197 \cdot T_{920} + 117,412 \cdot \frac{T_{817}}{T_{920}} + 22,734 \cdot \frac{(T_{817} - T_{920}}{T_{837}}$$

$$55,965 \cdot \frac{T_{817}}{T_{837}} + 8,987 \cdot \mu_{981} + 0,291 \cdot \mu'_{798} - 1,059 \cdot \mu'_{817} + 12,504 \cdot \mu''_{817}$$

The wavelengths chosen correspond to the more relevant features. For example, it was observed that the transmittance showed typically two peaks at 817 nm and 920 nm (Figure 3, bottom), the latter being relatively stable and the former changing appreciably in relation with the internal state of the fruit. Hence T_{817}/T_{920} was chosen as a candidate variable for the regression. The summary table of the *lm()* model allowed to restrict an initial set of candidates to the final set of 9 by using the p-values computed for each variable. All the variable in this model have p-value < 0.005.

To test the validity of the model, we calculated the predicted values and compared them to the observed values (figure 4).

In this study we have made a preliminary proof of concept that detection of internal defects in pomegranates is possible through transmittance spectroscopy. This is possible due to observable differences at specific wavelengths and also in the spectrum shape as a whole (see figure 5). The results are encouraging, but still limited. The universe of samples is small and dominated by rot fruit. Equal percentages of fruit in severity classes 1 to 5 is required to develop a more robust prediction model. Furthermore, and again due to the limited number of samples, an external validation was not performed. In any case, the multilinear regression model yielded a very good description of the data.

Acknowledgements

The authors acknowledge Luís Sabbo Lda. (Tavira, Portugal) for providing the fruit used in this study and FCT - Fundação para a Ciência e a Tecnologia, Portugal, for funding CEOT strategic project UID/Multi/00631/2013 (BI fellowship of A. Brázio) and Ana M. Cavaco through a post-doc fellowship (SFRH/BPD/101634/2014).

References

Clark, C. J., McGlone, V. A., & Jordan, R. B. 2003. Detection of Brownheart in 'Braeburn' apple by transmission NIR spectroscopy. Postharvest Biology and Technology 28(1): 87-96.

Han, D., Tu, R., Lu, C., Liu, X., & Wen, Z. 2006. Nondestructive detection of brown core in the Chinese pear 'Yali' by transmission visible–NIR spectroscopy. Food Control 17 (8): 604-608.

Khoshroo, A., Keyhani, A., Zoroofi, R. A., Rafiee, S., Zamani, Z., & Alsharif, M. R. 2009. Classification of pomegranate fruit using texture analysis of MR images. Agricultural Engineering International: CIGR Journal.

Magwaza, L. S. & Opara, U. L. 2014. Investigating non-destructive quantification and characterization of pomegranate fruit internal structure using X-ray computed tomography. Postharvest Biology and Technology 95: 1-6.

Nicolai, B. M., Beullens, K., Bobelyn, E., Peirs, A., Saeys, W., Theron, K. I. & Lammertyn, J. 2007. Nondestructive measurement of fruit and vegetable quality by means of NIR spectroscopy: A review. Postharvest biology and technology 46 (2): 99-118.

R Core Team (2014). R: A Language and Environment for Statistical Computing. R Foundation for Statistical Computing, Vienna, Austria. Available at https://www.R-project.org/

Savitzky, A. & Golay, M. J. 1964. Smoothing and differentiation of data by simplified least squares procedures. Analytical chemistry 36 (8) 1627-1639.

Simmons, E. G. 1967. Typification of Alternaria, Stemphylium, and Ulocladium. Mycologia 59 (1): 67-92.

Tziros, G. T., Lagopodi, A. L., & Tzavella-Klonari, K. 2008. Alternaria alternata fruit rot of pomegranate (Punica granatum) in Greece. Plant Pathology, 57 (2): 379-379.

Zhang, L., & McCarthy, M. J. 2012. Black heart characterization and detection in pomegranate using NMR relaxometry and MR imaging. Postharvest biology and technology 67: 96-101.

Tables and Figures

Table 1. Determination of the severity and extension of fruit internal rotting.

	Severity					Extension of the damage (%)				
	none	mild	medium	severe	extreme	0	25	50	75	100
Number of pomegranates	1	2	3	2	22	1	4	1	5	19

Table 2. List of variables used in the multilinear regression model.

	Normalised transmittance			μ_{SG}	μ'_{SG}		μ''_{SG}
Wavelength (nm)	817	837	920	981	798	817	817

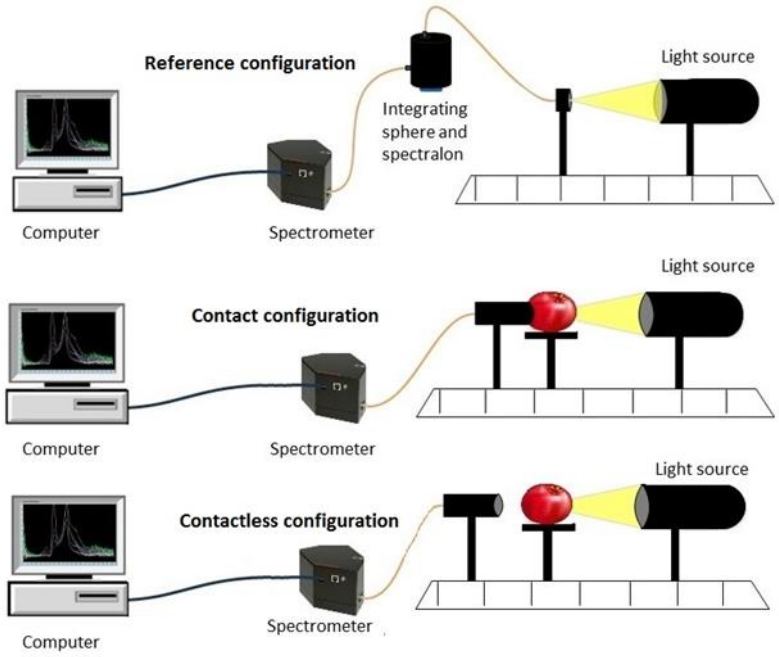

Figure 1. Optical setup. Top: setup for the reference measurement; middle: contact configuration; bottom: contactless configuration.

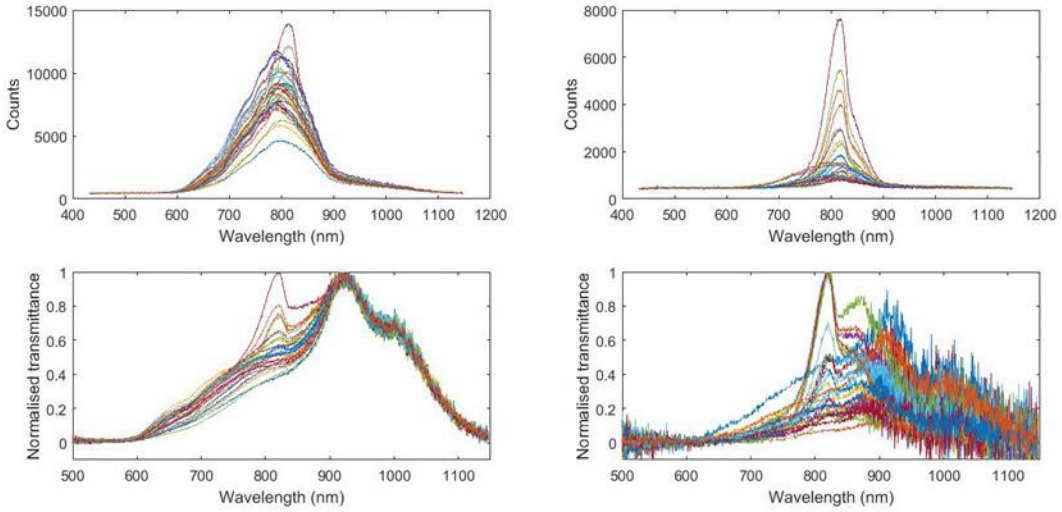

Figure 2. Raw spectra in the contactless configuration (top left), contact configuration (top right); Normalized transmittance spectra in the contactless configuration (bottom left), contact configuration (bottom right).

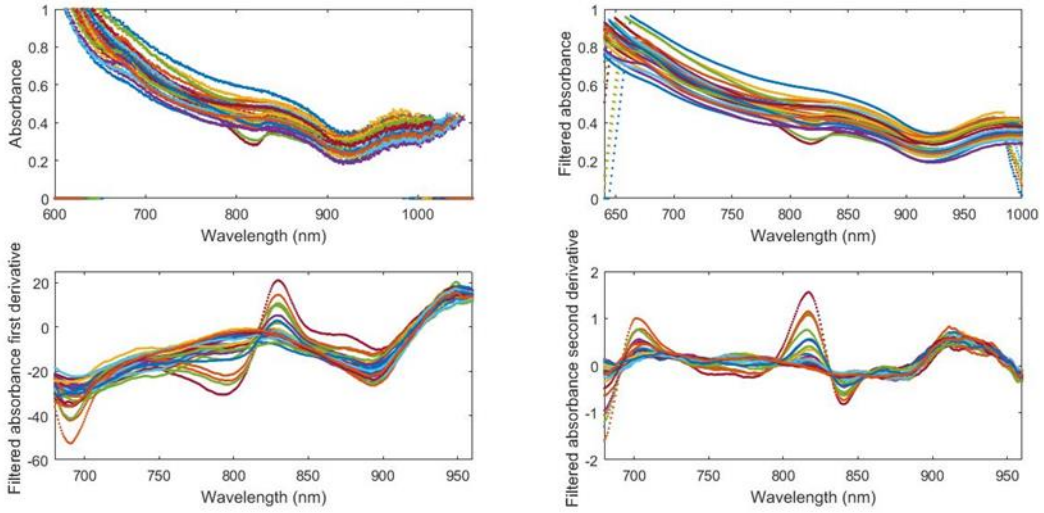

Figure 3. Absorbance spectra (top left), SG filtered absorbance spectra (top right), SG filtered absorbance first derivative spectra (bottom left) and SG filtered absorbance second derivative spectra (bottom right).

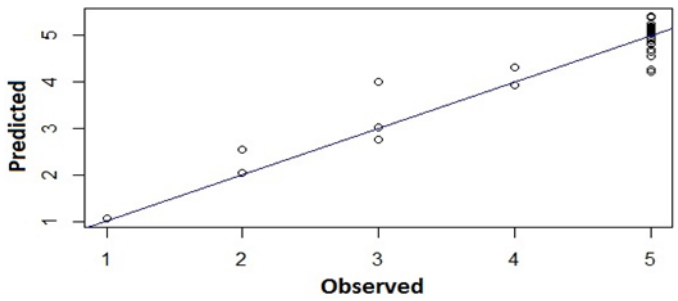

Figure 4. Predicted vs. Observed values of the severity of the internal damage.

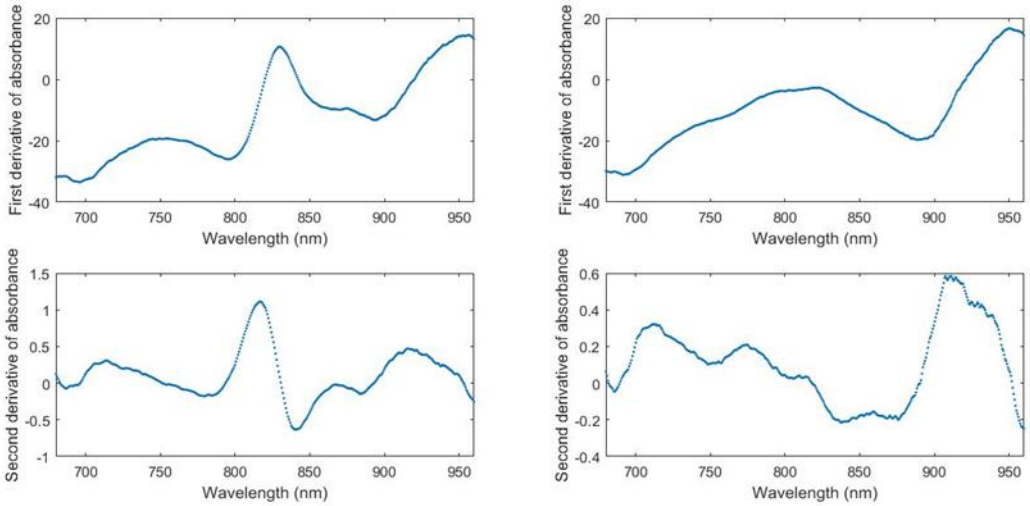

Figure 5. Comparison between two pomegranates: one with no internal damage (left) and another with extensive extreme damage (right).